Influence of Fixed-Pitch Tidal Turbine Hydrodynamic Characteristic on the Generator Design

S. Djebarri[1*#], J.F. Charpentier[2*], F. Scuiller[3*], M.E.H. Benbouzid[4#]

French Naval Academy, IRENav EA 3634,

Ecole navale BRCM BREST CC 600 - 29240 BREST Cedex 9 –

FRANCE

[1]sofiane.djebarri@ecole-navale.fr

[2]jean-frederic.charpentier@ecole-navale.fr

[3]franck.scuiller@ecole-navale.fr

#*University of Brest, EA 4325 LBMS*

Rue de Kergoat, 29200 Brest

FRANCE

[4]mohamed.benbouzid@univ-brest.fr

Abstract— **This paper deals with the global design of direct driven permanent magnet (PM) generator associated with fixed-pitch turbine for tidal energy generation. A global design approach of the generator design is proposed which takes into account the tidal site energy potential, the turbine hydrodynamic characteristic, the converter characteristics and an original power levelling control strategy. Because the considered turbine is without variable pitch control, the power levelling strategy is only based on torque/speed electrical control of the generator. Applying this global design process, it can be shown that the hydrodynamic characteristic (shape of the power coefficient curve (C_p)) have strong effects on the final design of the generator. The aim of the presented work is to evaluate this influence. Two C_p curves are considered for the same resource, turbine diameter and rated power. The obtained designs are compared in terms of cost and mass of the active parts and power factor of the generator. In the last part of the paper, the qualitative influence of the shape of the different parts of the C_p curve on the generator design is discussed.**

Keywords—— **Tidal turbine, fixed-pitch turbine, direct-driven generator, generator design, hydrodynamics**

I. INTRODUCTION

A. Tidal Energy System Analysis

Tidal energy is a renewable source of energy, its potential is easily predictable many years in advance. This energy is generated by the ocean currents which results from the contribution of the gravitational forces of the moon and the sun on the oceans (tides) [1]. The total potential of this energy resource is estimated to 450 TWh/year, with about 24 TWh/year on the European coasts. In Europe this resource is distributed mainly between UK with 48 %, France 42% and Ireland 8% [2]. Therefore, it constitutes a good alternative to complete the other renewable energy resources for power generation. In addition, the predictable nature of this energy resource is highly interesting for the grid connection of marine current turbines. This aspect facilitates the management of the produced electricity. Other advantages can make this energy resource interesting to be exploited, such as reduced environmental impact, low visual pollution and noise exposure for the population [3].

The Tidal Stream Turbines (TSTs) are underwater systems and extract the kinetic energy of water flow [1]. This is why TSTs systems can be similar in principle to the systems used in wind turbines generation, and can include the following elements:

• The turbine: according to literature [4,5], the horizontal axis turbines are mainly used in the first prototypes of industrial TSTs which are currently in test or in development. It can include variable or fixed pitch blades. The blades orientation mechanism allows the control of the turbine power by varying the blades pitch angle. However, this mechanical control system increases the complexity of the tidal generation system and increases the failure probability of the TST. It should be noted that for an offshore application and particularly for tidal power generation, enhancing reliability and reducing maintenance are key futures for sustainable and cost-attractive exploitation of marine currents [3].

• A gearbox can be used to increase the drive speed of the generator. Nonetheless, this element causes a major part of failures and maintenance requirements [6]. This is why direct drive system where the generator is directly driven by the turbine without using gearbox can be interesting solution [4,5].

• The generator is an important element in the drive train as it realizes the energy conversion from mechanical energy to electrical power. In direct-drive systems, low speed permanent-magnet (PM) machines are mainly used. In this case, the rotational generator speed is typically below 50 rpm for high power turbines (TSTs).

• The converter allows the control of the generator and the power regulation before its injection to the grid. Several architectures of power converters are possible for TSTs application [7]. Back to back IGBT PWM converters are one

the more considered options for high power systems (more than 100 kW)

• A storage system, can be used in particular configurations for smoothing the electrical power before its injection into the grid [8].

B. Studied System and Proposed Study

Referring to literature [9], the gearbox and the blades variable pitch system are the main sources of failure and maintenance in wind turbine application. With tidal power generation, the maintenance is a key future because it is extremely difficult to operate on immersed seawater TSTs. In addition the maintenance adds significant additional costs. In order to reduce maintenance requirements, a simple architecture of the drive train is considered in this study (see figure 1). This system which uses a direct drive PM generator is considered. The turbine is a fixed pitch turbine. This kind of system is used in some major industrial projects as for example in Open-Hydro or Voith Hytide projects [4]
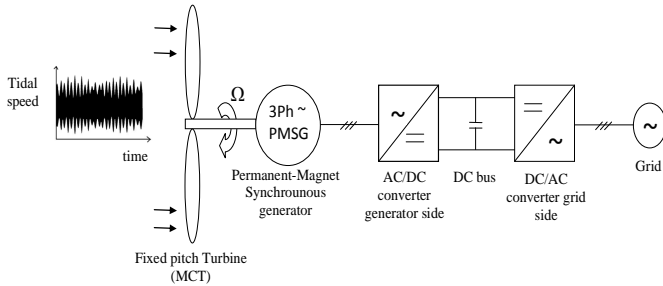

Fig. 1. Marine current turbine drive train, with direct-drive generator and fixed-pitch blades.

Power limitation strategy is interesting to a cost-attractive sizing of the electrical parts of the energy conversion chain. It avoids a significant over sizing of the electrical elements. When the turbine has variable pitch blades, the power limitation strategy is achieved mechanically by varying the blades pitch angle. For fixed pitch turbines, the power limitation control have to be electrically carried out by torque and speed control of the generator. A strategy to be able to make this power limitation possible is to use over speed flux weakening operations as proposed in [10]. In this paper we use a specific design methodology of a radial flux permanent magnet (RFPM) generator taking into account this specific control strategy of power limitation [11]. A global design approach of the generator to take into account these specific requirements is described. This methodology takes into account the tidal site energy potential, the control strategy, the power converter constraints and the turbine characteristic (C_p curve). In this design process, several models are associated in an under constraints optimization process. It takes into account: the control strategy, the generator specifications, the energy resource characteristic, the turbine power coefficient (C_p) law and the converter voltage and current constraints. Using this approach the shape of the C_p curve has a strong

influence on the final results. The aim of the paper is to evaluate this influence on the generator design results. This global design methodology is described in the second part of the paper. In the third part, two designs are achieved according to the given methodology for two turbine characteristics and the results are discussed. It will allow us to analyse how the shape of the different parts of the turbine power coefficient curve (width of the growing part and the descending part, maximal value) will impact the generator and drive design.

II. DESIGN METHODOLOGY

A. Tidal Resource Modelling and Analysis

In this study, Raz de Sein tidal site, France, is considered thanks to its high tidal current velocity and favorable location near the coasts. The GPS coordinates of the studied site are ($\varphi_B = 48°02'42''$, $G_B = 4°45'45''$). The used data consist of the velocity values for each hour during a tidal period of 8424hours [1]. The considered period is sufficiently significant to have a good idea of the tidal current variation in the lifetime of the system. The tidal velocity is here varying between -2.75m/s to 3.63m/s. Figure 2 show the velocity variation during the considered period. This time series can be determined based on tidal current data from SHOM (French Navy Hydrographic and Oceanographic Service). In all the study the flow is assumed to be steady and the turbulence and sea state influence are neglected. If the tidal speed range is divided by n interval and the speed in the ith interval is v_i, Fig. 3 represents the occurrences OCC_i (number of hours) corresponding to the ith tidal speed interval in the considered tidal period. OCC_i corresponds to the number of hours in the ith tidal interval around the speed v_i.

Knowing the occurrence of the tidal velocity, it is possible to calculate the corresponding energy potential density (Wh/m^2) by the following formula.

$$E_p^i(v_i) = \frac{1}{2}\rho_{water}\left|v_i^3\right| \times OCC_i(v_i) \tag{1}$$

Where E_p^i is the energy potential given in (Wh/m^2), ρ_{water} is the water density, v_i is the tidal speed, and OCC_i is the occurrences at speed v_i.
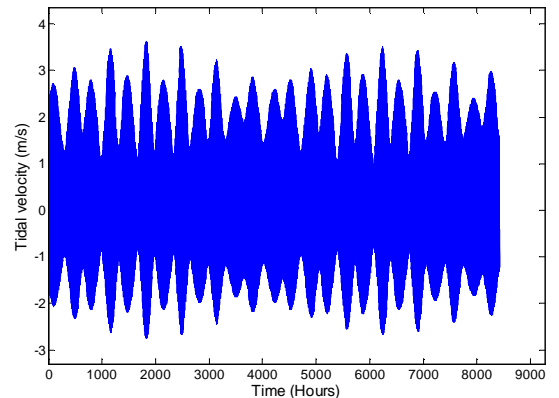

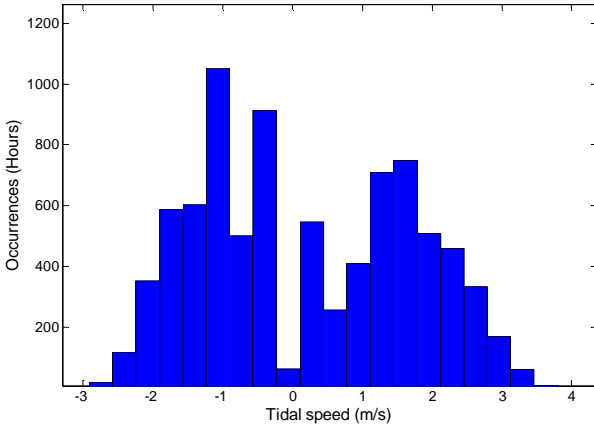Fig. 2. Tidal velocity in Raz de Sein site, France

Fig. 3. Occurrences (OCC$_i$) versus tidal velocity (v_i) : France : the data corresponds to the time serie of fig 2 (8424 hours)

Figure 4 illustrates the energy density potential by square meter of turbine swept area distribution deduced from (1)
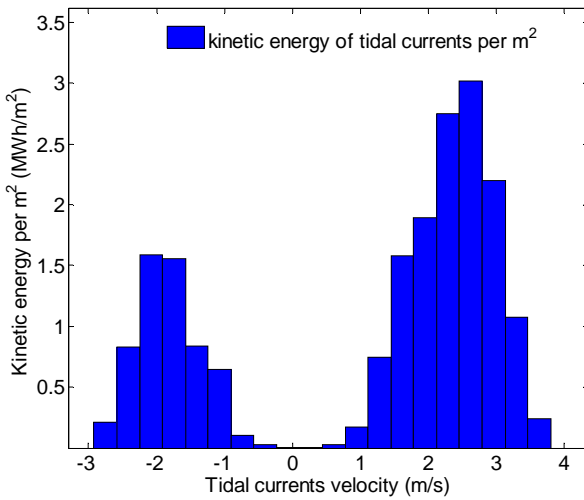

Fig. 4. Energy potential distribution in Raz de Sein site, France : the data corresponds to the time serie of fig 2 (8424 hours)

B. Turbine modelling

If the energy potential of the tidal site is known for each speed value, it is possible to calculate the turbine extractable energy by

$$E^i(v_i) = E_p^i(v_i) \times S_{turbine} \times C_p(\lambda(v_i)) \qquad (2)$$

Where $S_{turbine} = \pi D_{turbine}^2 / 4$ is the turbine blade swept area and $C_p(\lambda(v_i))$ is the power coefficient given for a Tip-Speed-Ratio (TSR) $\lambda(v_i)$ which is determined for each speed value v_i.

The turbine is characterized by a C_p (power coefficient) law. For a fixed-pitch turbine this factor is considered to depend only of of the Tipp Speed Ratio, λ. Tip Speed Ratio is defined as the ratio between the blades peripheral speed to the tidal current speed.

$$\lambda = \frac{\Omega \times (D_{turbine}/2)}{|v|} \qquad (3)$$

Where Ω (rad/s) is the generator rotational speed, $D_{turbine}$ (m) is the turbine diameter and v (m/s) is the tidal current speed. In this study, C_p curves are fitted by an interpolation function. In all the study the used velocities are considered to be in the same direction as the turbine axis and to be able to extracted in similar way in the two (ebb and flow) directions (use of a symmetrical turbine or use of a yaw system).

As an example the figure 5 presents the C_p data of an experimental underwater turbine prototype which is studied in [11] and the corresponding interpolation function. In this example the C_p curve reaches his maximal value $C_{pmax} = C_p(\lambda_{opt}) \approx 0.46$ for $\lambda_{opt} \approx 6$.

In the presented example case, the used interpolation function is given by eq (4). This C_p curve is used here to illustrate the design methodology. For the results given in section III, two others C_p curves with the same C_{pmax} are considered.

$$\begin{cases} C_p(\lambda) = 0.0195\lambda^2 \left(1.3172e^{(-0.3958\lambda+1.539)} - 0.0867\cos(0.4019\lambda - 5.6931)\right) \\ \lambda \in [0 \quad 11.8] \end{cases} \qquad (4)$$
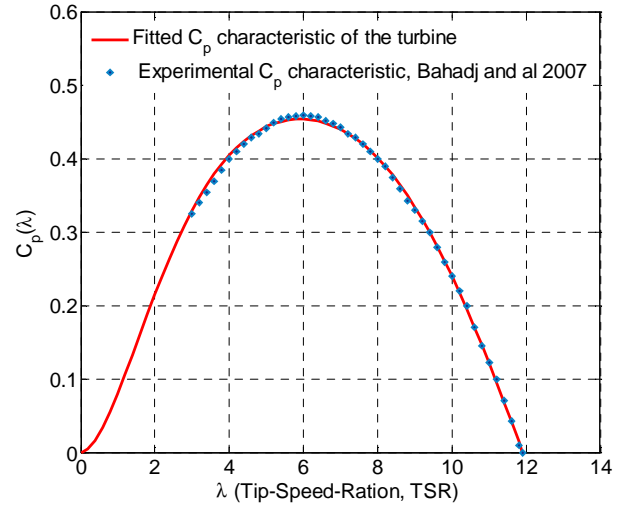

Fig. 5. Cp law of the turbine presented as an example.

C. . Control Strategy

In this section, the turbine control strategy is defined from the tidal speed characteristic and the turbine specifications.

For a given value of Ω and v the turbine extracted power is calculated by (5)

$$P_{turbine} = \frac{\pi}{8}\rho_{water}D_{turbine}^2 C_p(\lambda)\left|v^3\right|$$ (5)

In Fig. 4, it can be seen that the tidal current energy potential is very low at high tidal speed. It is then obvious that the limitation power strategy is necessary to avoid a power oversizing of the electrical conversion chain. Figure 6, particularly illustrates P^* that denotes the turbine reference operating power (control strategy). It is calculated by (6). This power limitation strategy is illustrated by Fig.6 and is described as follow.

$$P^* = \begin{cases} \dfrac{\pi}{8}\rho_{water}D_{turbine}^2 C_{pmax}\left|v^3\right| & \text{if } |v| \le v_{Lim} \\ P_{Lim} & \text{if } |v| > v_{Lim} \end{cases}$$ (6)

For $v < v_{lim}$, the turbine speed is, of course controlled by the converter to reach the optimal value of the TSR, λ which corresponds to C_{pmax} (C_p value is considered to depend only of the TSR, λ)
P_{Lim} is the limitation value of the turbine power (i.e. the rated power of the generator). If P_{Lim} is known, it is obviously possible to determine the limit tidal speed v_{Lim} (i.e. the rated tidal speed) where the limitation power strategy is applied. It is calculated by

$$v_{Lim} = \sqrt[3]{\frac{P_{Lim}}{\left(\dfrac{\pi}{8}\rho_{water}D_{turbine}^2 C_{pmax}\right)}}$$ (7)

The base rotation speed Ω_b (rad/s) of the generator is then deduced as below

$$\Omega_b = \frac{\lambda_{opt}v_{Lim}}{\left(D_{turbine}/2\right)}$$ (8)

Then the base rotational speed in rpm is:

$$N_b = \Omega_b \times \frac{60}{2\pi}$$ (9)

The maximal speed (given at the limit operating point of Fig. 6) is defined by

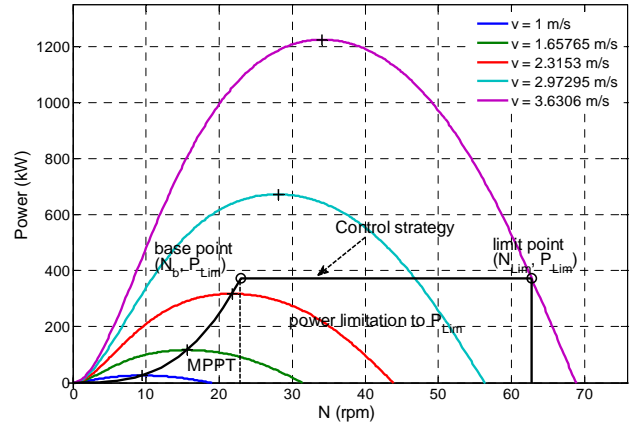Fig. 6. Extracted power and used control strategy.

$$\Omega_{Lim} = \frac{\lambda_{Lim}v_{Lim}}{\left(D_{turbine}/2\right)}$$ (10)

And

$$N_{Lim} = \Omega_{Lim} \times \frac{60}{2\pi}$$ (11)

Where λ_{Lim} is calculated by solving the following equation.

$$C_p(\lambda) - \frac{P_{Lim}}{\left(\dfrac{\pi}{8}\rho_{water}D_{turbine}^2\left|v_{max}^3\right|\right)} = 0$$ (12)

Equation (13) gives the extracted energy by the turbine corresponding to the C_p law of fig.5 considering the chosen tidal site and adopting the described limitation power strategy.

$$E_{extracted} = \sum_{i=1}^{n} P^*(v_i) \times OCC_i(v_i)$$ (13)

Figure 7 gives the extracted energy when the limitation power rate is varying. P_{Lim} is varying from 5% to 100% of the maximum power that can be extracted by the considered turbine ($P_{max} = P(C_{pmax},v_{max}) = 1245$kW in the studied case). In this case the considered turbine has a diameter of 12m and begins to operate at a tidal speed of 1m/s (the turbine is stopped under 1m/s speed of water current). It clearly shows that limiting the power at high tidal speed to 30% of the maximum turbine power is enough to extract 87.5% of the total extractible energy. Then the limitation power is set to $P_{Lim} = 374$kW. According to this control strategy the turbine operates until 7864hours with MPPT control and 560hours in power limitation mode. Therefore 75% (656MWh) from the total extracted energy (884MWh) is extracted during the MPPT control mode and 25% (228MWh) during the limitation power mode. It can be noticed that in this case the amounts of extracted energy for a given turbine diameter do not depend on the shape of the C_p curve. These amounts

depend only of the maximal value of C_p, C_{pmax}, of the value of P_{lim} and the of the efficiency of the drive train.

The torque setpoint characteristic that the generator-drive system should develop during an operating rotational speed cycle can be deduced from the P^* $V.S.$ N curve using eq.(14).

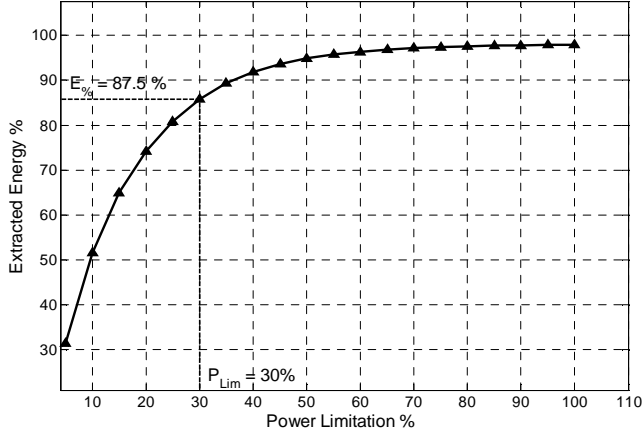$$\Gamma^* = \frac{P^*}{N \times (2\pi/60)} \tag{14}$$

Fig. 7. Extracted energy rate versus power limitation rate.

Figure 8 gives the torque characteristic that the generator should be able to develop in the presented example (corresponding to the C_p curve of fig. 5.) This torque characteristic is then introduced as a specification to design the PM generator. It can be observed from this figure that the design torque characteristic can be introduced as two design points. The first one is the base point where the machine must develop the base torque Γ_b (it corresponds to the maximum torque) at base speed N_b. The second one is an over speed limit point, this point is introduced as a constraints in the generator design specifications. It traduces the torque Γ_{Lim} that the generator should be able to produce at the maximum rotational speed N_{Lim} of the turbine during an operating cycle.

D. Introducing Power Converter Limits

In our methodology the power converter constraints are taken into account. The converter is considered as a double bridge IGBT back-to-back one [5,10]. The grid side converter voltage is set to $V_{grid} = 690V$ (rms). This voltage corresponds to a typical output voltage of offshore wind turbines [13]. Then the maximum generator phase voltage allowed by the power converter is here set to $V_{max} = V_{grid}$. V_{max} corresponds to the power converter input voltage.

E. Generator calculation method

The generator is a radial flux permanent magnet machine and it is modeled considering the geometry illustrated in Fig. 9. The models used for generator design consist mainly on electromagnetic model coupled with a thermal one as

described in [11],[14],[15]. These models allow calculating the electromagnetic torque, the electrical power, the electrical losses and the thermal behavior over the speed range operating cycle.

The generator design is formulated as an optimization problem that consists on minimizing the active parts costs function $C(x)$ under linear and nonlinear constraints. This objective function takes only into account the magnets, copper, and iron sheets material costs (used cost by kg are given in table I). x is here the geometry variables. The constraints consist of:

– Equality constraint on the generator torque at the base speed $\Gamma_b(\mathbf{x},\Omega_b)$.
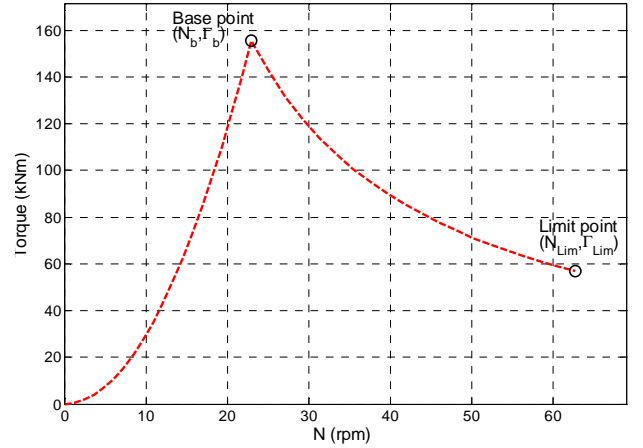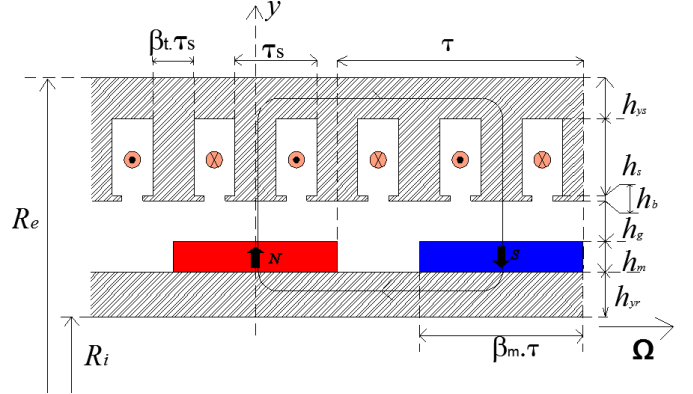

Fig. 8. Generator torque setpoint specification.

Fig. 9. Geometry of the RFPM generator, R_e is the outer magnetic radius, R_i is the inner magnetic radius, h_{yr} is the rotor yoke height, h_m is the magnet height, h_g is the air gap height, h_s is the slot height, h_{ys} is the stator yoke height, β_m is the magnet-to-pole width ratio, τ_s is the slot pitch width, β_t is the tooth-to-slot width ratio.

– Equality constraint on the generator phase voltage $V(\mathbf{x},\Omega_{Lim})$. This constraint is introduced by the power converter input voltage.
  These two constraints are introduced as equality constraints to minimize the sizing of the generator and the converter.
– Inequality constraint on torque that the generator/converter set is able to provide at the limit operating speed. Thereby

the generator torque $\Gamma_{Lim}(\boldsymbol{x},\Omega_{Lim})$ at maximum speed Ω_{Lim} must be higher than the required torque at this speed. This constraint specifies the speed range where the generator/converter can operate at constant maximal power. Considering Flux weakening operations of PM machines this constraint is mainly associated to the ratio between the stator armature flux which is related to cyclic inductance value and the PM flux. That means that if a very large range of speed have to be reached, the power factor of the generator will decrease [16]

- Inequality constraint on the electrical power factor *FP*. The power factor $FP(\boldsymbol{x},\Omega_b)$ at base speed must be higher than a fixed minimal power factor value FP_{min} This constraint is introduced to avoid a very low power factor at low speed.
- Inequality constraint on the electrical efficiency. The generator electrical efficiency $\eta_{elec}(\boldsymbol{x},\Omega_b)$ must be higher than a minimal set value $\eta_{elec,min}$. This constraint is defined to avoid very low generator electrical efficiency.
- Inequality constraint on the maximum generator temperature. This constraint ensures the thermal feasibility of the generator. It is defined as the maximum temperature $T(\boldsymbol{x},\Omega_b)$ in conductors at base speed. The temperature $T(\boldsymbol{x},\Omega_b)$ should be lower than the maximum temperature T_{max} allowed by the conductors class thermal insulation.
- Inequality constraint on the maximum magnetic field $H_{max}(\boldsymbol{x})$ in the magnets. The magnetic field in magnets is calculated by considering the worst case where the flux created by stator currents is in opposition with the magnets flux. Therefore to avoid the magnets demagnetization, the value of magnetic field should be lower than the magnets coercive field H_{cj}.
- Linear inequality constraints on the generator geometry variables. They are introduced in the optimization problem to ensure generator feasible geometry.

This optimization problem is summarized by Eq. (15). It is performed under the Matlab® optimization toolbox with the *fmincon* algorithm. To achieve this optimization a set of common parameters used in this study to define the constraints are given in Table I. In equation 15 *LB* and *UB* are respectively the lower and upper bound of the geometrical variables.

$$
\mathbf{x}^{*}=\min_{\mathbf{x}\in\mathbf{X}}\left\|C(\mathbf{x})\right\|
$$

$$
\begin{cases}
\Gamma(\mathbf{x},\Omega_b)-\Gamma_b^{*}=0 \\
V(\mathbf{x},\Omega_b)-V_{max}=0 \\
-\Gamma(\mathbf{x},\Omega_{Lim})+\Gamma_{Lim}^{*}\leq 0 \\
-PF(\mathbf{x},\Omega_b)+PF_{min}\leq 0 \\
T(\mathbf{x},\Omega_b)-T_{max}\leq 0 \\
\left|H_{max}(\mathbf{x},\Omega_b)\right|-\left|H_{cj}\right|\leq 0 \\
-\eta_{elec}(\mathbf{x},\Omega_b)+\eta_{elec_{min}}\leq 0 \\
LB\leq\mathbf{x}\leq UB
\end{cases}
\qquad (15)
$$

TABLE I. GENERATOR SPECIFICATIONS.

Generator external diameter	$D_{generator}$	3	m
Power limitation (rated power)	P_{lim}	374	kW
Power converter input voltage	V_{max}	690	V(rms)
Minimal generator electrical efficiency	$\eta_{elecmin}$	96	%
Maximum generator temperature	T_{max}	100	°C
Magnets coercive field	H_{cj}	10^6	A/m
Magnet cost		115	$/kg
Iron cost		1	$/kg
Copper cost		7.8	$/kg

III. INFLUENCE OF THE TURBINE CHARACTERISTICS ON THE GENERATOR AND DRIVE DESIGN

A. Comparison of generator designs for two different turbines

According to the described methodology the generator is designed and the obtained generator geometry parameters are calculated for two different 12m diameter turbines. These two turbines are characterized by two very different $C_p(\lambda)$ curves. The maximal C_p values of the two turbines are identical ($C_{pmax}=0.44$) and the used control strategy is identical. It is also supposed that the two turbines will begin to extract energy only when the tidal speed is over 1m/s and that the value of power which corresponds to the base speed (power limitation) is identical.. That means that a same $P^*(v)$ is used in the two cases (considering eq. 6 the maximal power which corresponds to the power limitation is reached for the same speed, v_{lim}). With these assumptions that means, considering the methodology presented in previous part, that the amount of energy extracted by the two systems with the considered strategy is identical. The two turbine $C_p(\lambda)$ laws are shown in fig.10.
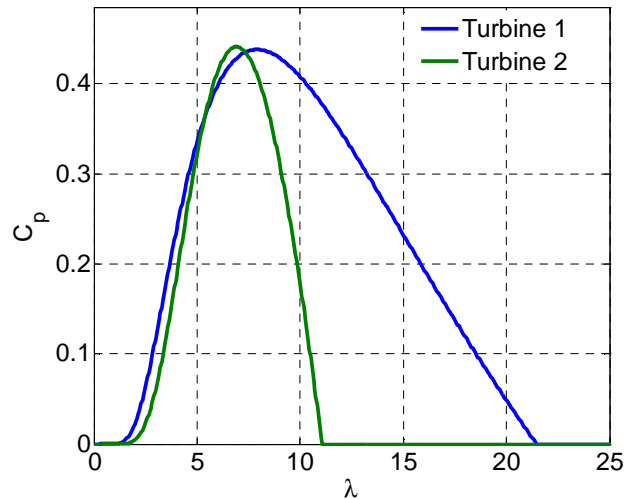

Fig. 10. Turbine $Cp(\lambda)$ laws used for the comparizon.

These two turbines characteristics correspond to two different turbine designs which have been studied in literature. The first one (turbine 1) is extracted from [17] and is characterized by a maximal power coefficient of 0.44 reached for an optimal Tip Speed Ratio $\lambda_{opt}=7.9$. The free speed

(speed where the C_p is null) corresponds, in this first case, to a TSR $\lambda_{max}=21.5$. An interpolation of this first turbine C_p curve is given by eq. (16). The second one (turbine 2) is extracted from [18] and is characterized by a maximal power coefficient of 0.44 reached for an optimal Tip Speed Ratio $\lambda_{opt}=6.9$. The free speed (speed where the C_p is null) corresponds, in this second case, to a TSR $\lambda_{max=}11$. An interpolation of the C_p curve of this second turbine is given by eq. (17). In equations (16) and (17) β is the pitch angle. In the considered study, the turbine is considered to be a fixed pitch one and β is considered to be null. Considering the curves of Fig.10, two main differences can be seen. In a first hand, the turbine speed corresponding to the C_{pmax} for a given value of current speed (or for a given power at MPPT) will be greater for the first turbine than for the second one. That means that the rated torque which corresponds to the base speed operating point (operating point corresponding to v_{Lim}) will be lower in the first case. In the other hand this first turbine C_p shape is more flat than the second one, that means that the range of rotating speed in the first case will be larger than in the second case.

$$\begin{cases} C_p\left(\lambda,\beta\right)=0.22\left(\dfrac{116}{\lambda_i}-0.48\times\beta-5\right)e^{\frac{12.5}{\lambda_i}} \\ \dfrac{1}{\lambda_i}=\dfrac{1}{\lambda+0.008\times\beta}-\dfrac{0.0035}{\beta^3+1} \end{cases} \quad (16)$$

$$\begin{cases} C_p\left(\lambda,\beta\right)=0.22\left(\dfrac{151}{\lambda_i}-0.58\times\beta-0.002\times\beta^{2.14}-13.2\right)e^{\frac{-18.4}{\lambda_i}} \\ \lambda_i=\dfrac{1}{\dfrac{1}{\lambda-0.02\times\beta}-\dfrac{0.003}{\beta^3+1}} \end{cases} \quad (17)$$

The C_p laws given in figure 10 and eq 16 and 17 allows to determine the power VS speed (P*(N)). These two power charcteristics are different and are given in fig. 11 and fig.12
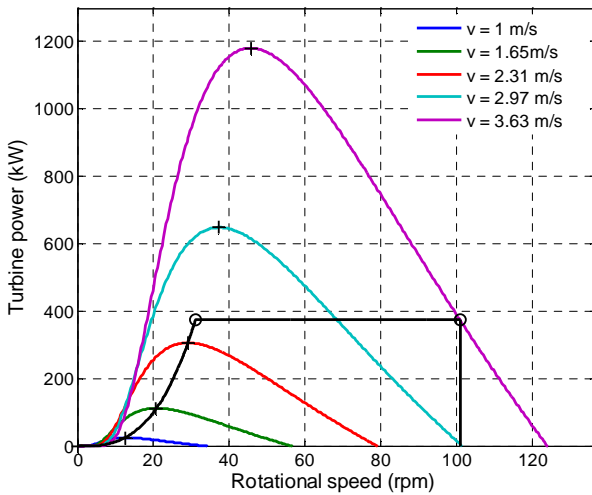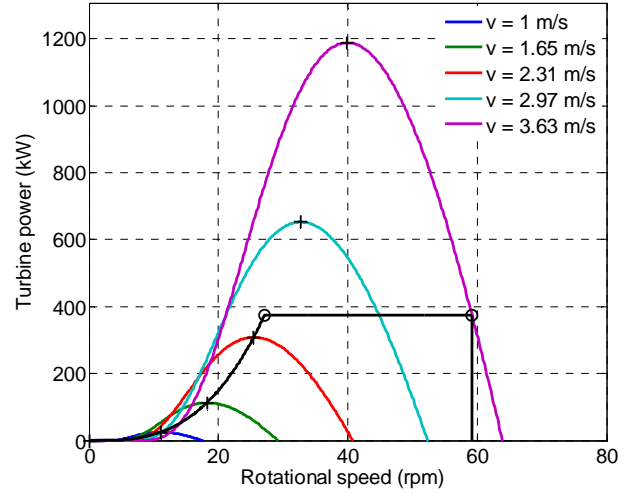

Fig. 11. Power characteristics for the first turbine

Fig. 12. Power characteristics for the 2nd turbine (P VS N).

From these power curves the torque VS speed specifications can be easily calculated. These torque VS speed characteristics are shown in Fig. 13 and allow to define for each case the two design points which are introduced as constraints in the optimisation problem described by eq (15)
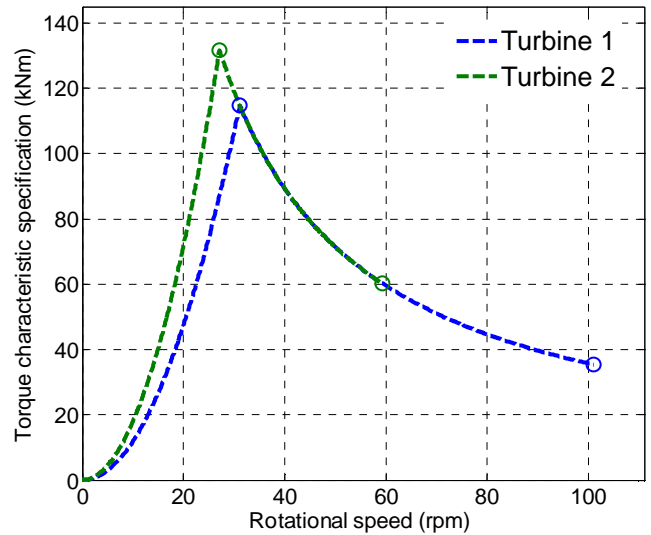

Fig. 13. Torque characteristics for the two turbines.

For each of the two studied cases, several optimization has been processed (by the previously presented method (Eq. (15)). The problem has been solved for different values for the constraint related to the electrical power factor. The presented results corresponds to the results obtained for the higher value of the power factor where a solution can be found which satisfy the other constraints (and particularly the constraints related to torque characteristics). It means that the presented solutions are those which minimize both the cost of the generator active part and the sizing of the converter.

Table II gives the main geometric parameters of the two designed generators. Figures 14 to 15 shows the torque/speed characteristics that the designed generators associated with their converters are able to reach in steady state. The figure 14 corresponds to the generator designed for turbine 1 and figures 15 corresponds to the generator designed for turbine 2. In these figures these electromechanical characteristics are compared with the specified torque curves of Fig. 13. In both cases the characteristics of the generator are over the specified torque/speed characteristics.

This result implies that the electrical power limitation strategy at high tidal speed can be performed only by controlling the two converter/generator/turbine sets according to the developed methodology.

TABLE II. DESIGNED GENERATORS MAIN PARAMETERS.

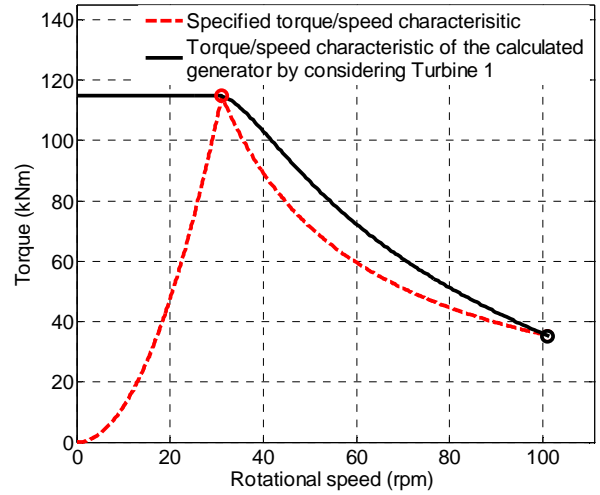|		Generator for turbine 1	Generator for turbine 2	
J	Current density	3.345	2.91	A/mm²
A_L	Electrical load	51416	45821	A/m
B_1	First harmonic of the Air gap flux density	0.647	0.609	T
p	Pair pole number	84	79	-
ncd	Number of conductors in series per slot per phase	4	4	-
m	Phase number	3	3	-
S_{pp}	Slot number per pole per phase	1	1	-
k_f	Slot fill factor	0.5	0.5	-
k_{b1}	Winding coefficient given at first harmonic	1	1	-
R_i	Inner radius	1.35	1.35	m
R_e	Outer radius	1.445	1.448	m
R_s	Stator bore radius	1.3714	1.3723	m
L_m	Active length	41.3	51.5	cm
β_m	Magnet to pole width ratio	2/3	2/3	
β_t	Teeth pitch ratio	49.12	49.6	%
h_{ys}	Stator yoke thickness	1	1.05	cm
h_{yr}	Rotor yoke thickness	1	1.05	cm
h_s	Slot height	5.9	6.1	cm
h_m	Magnet height	5.9	6.1	mm
h_g	Air-gap thickness	5.4	6.22	mm
FP	Reached electrical power factor (at base speed)	0.8	0.84	-

Fig. 14. Torque characteristics for the generator/converter designed for turbine 1.
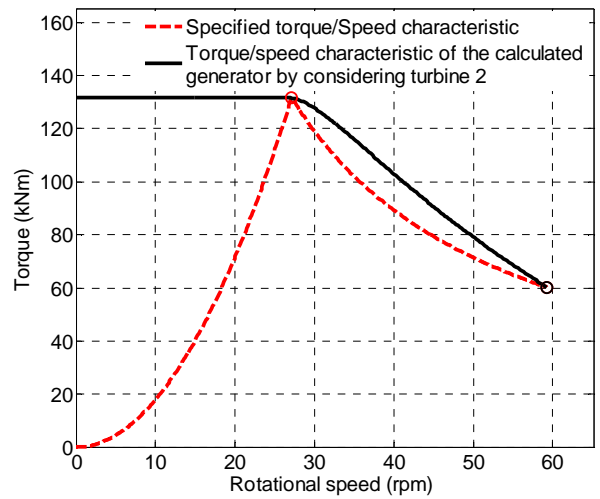

Fig. 15. Torque characteristics for the generator/converter designed for turbine 2
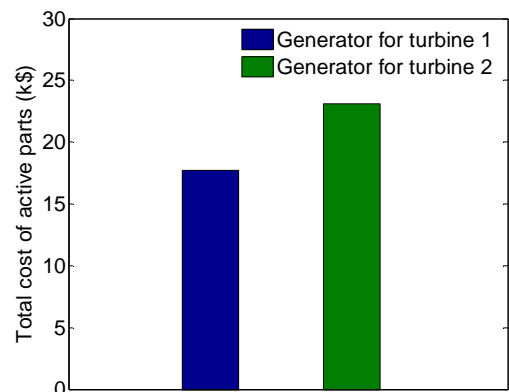

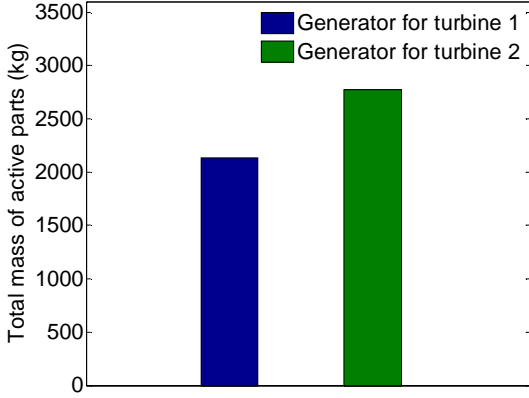Fig. 16. Cost of the active parts of the two generators.

Fig. 17. mass of the active parts of the two generators.

Fig. 16 and 17 gives a comparison of the cost and the total mass of the active parts for the two designed generators. Figure 18 gives the comparison of the power factors of the two generators. It can be noticed that the generator designed for the turbine 1 is characterized by a lower mass and cost of active parts than the generator designed for the turbine 2. It can be explained because the required maximal torque to apply the power strategy is higher for turbine 2 than for turbine 1 because the base speed is higher (higher value of λ_{opt}). Indeed, he maximal torque that the generator has to develop in steady state under thermal constraints is in first order directly linked to the active parts volumes. The increase of base speed of 14% leads to a reduction of about 23% of the cost and mass of the active parts.
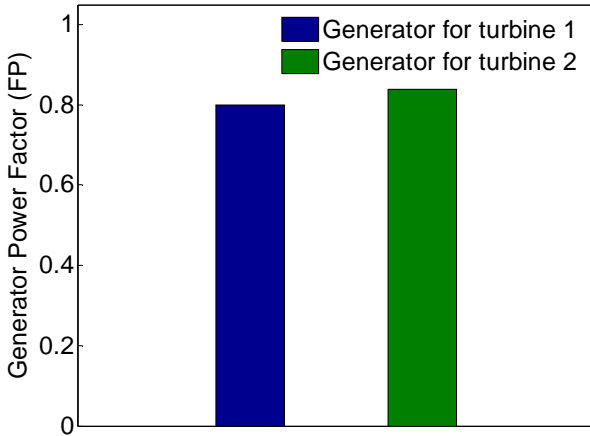

Fig. 18. Power factors the two generators.

Considering the power factors for the two designs shown in Fig.18 it can be noticed that the generator designed for turbine 1 has a lower power factor (*FP=0.8*) than the generator designed for turbine 2 (*FP=0.84*). This fact can be explained because a higher ratio between armature flux and PM flux is required for flux weakening operations to be able to reach the larger range of speed associated with the turbine 1. This lower power factor leads to an oversizing of the converter rated current and to over costs related to the converter designs.

This larger required range of speed will probably also lead to stronger mechanical constraints on the turbine and the drive train which have to be designed to operate securely at a speed, N_{lim}, which is around three times the speed corresponding to the base point (N_b). For turbine 2 this range of speed is strongly reduced which leads to lower constraints on the power factor which can be reached and lower mechanical constraints.

B. Qualitative analysis on the influence of the hydrodynamic characteristic of the turbine on generator design.

In Fig. 19, the general shape of a turbine C_p curve is presented. This curve can be divided in two area. The first one (A Area) corresponds to the growing part of the C_p curve and the second one (B Area) to the descending part of the C_p curve.
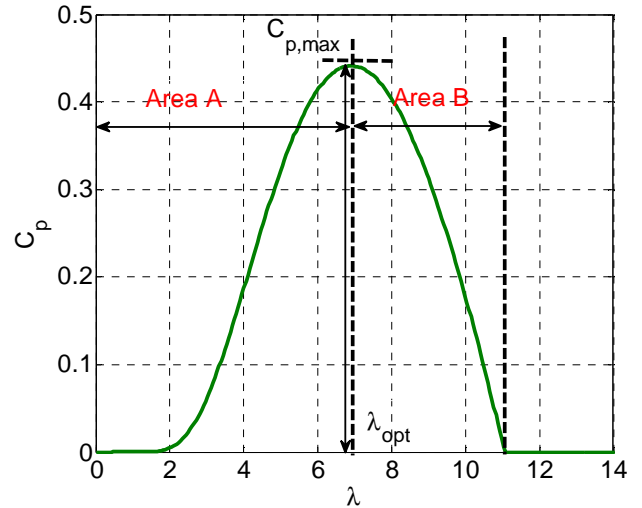

Fig. 19. Analysis of the shape of the C_p law.

The curve is also characterized by its maximal value C_{pmax} obtained at an optimal TSR, λ_{opt}. Of course to extract optimally the resource potential for a given turbine diameter, the value of C_{pmax} must be maximized.

Some trends can be underlined to assess the influence of the turbine Cp curve on the generator design:

In one hand, increasing the width of "A Area" (increasing the value of λ_{opt}) allows to decrease the maximal torque that the generator have to manage in steady state by increasing the power limitation rotating speed (base speed). This torque, is in first order, proportional to the generator active part volume. So a high value of λ_{opt} allows minimizing the active part global costs. In the other hand, the "B Area" must be narrower as possible if the presented power limitation by over speed operation is used. Indeed, if the width of this area is reduced,

it allows reducing the constant power speed range and also the electrical constraints related to flux weakening operations. This constraint is directly related to the value of the cyclic inductance in per unit. That means that the generator/converter set will be designed to operate at a higher power factor (in the rated point) which leads to a more advantageous sizing of the converter. It will also reduce the mechanical constraints in the turbine and the drive train related to high speed.

IV. CONCLUSION

This paper aims to assess the influence of the turbine characteristics on the generator design constraints. The studied systems are direct-drive permanent magnet generator associated with a fixed-pitch turbine and back to back IGBT PWM converter for tidal generation. A global design methodology is proposed which takes into account the resource characteristic, the turbine law, the generator specifications, a specific power limitation control strategy and the converter constraints. The used control strategy is only based on the generator control adopting a flux weakening approach to limit the power by over speed operations. With this design approach, the shape of the power coefficient curve of the turbine has a strong influence on the generator design because it impacts on both the rated torque of the generator and the flux weakening constant power operation speed range. This speed range impacts directly the power factor of the generator. This power factor is directly linked to the sizing of the converter. Two C_p curves with different shapes and the same maximal values of power coefficient are used. These curves are considered to characterize 12 m diameter fixed pitch horizontal axis turbines. Two corresponding generator designs have been calculated with the proposed global method and the results are discussed. This study allows determining qualitative general rules on the influence of the turbine characteristics on the design of the converter/generator set. However in all the study the flow is assumed to be steady and the turbulence and sea state influence are neglected. Further works can be conduces to assess the influence of such disturbance on the results.

REFERENCES

[1] S. Benelghali, R. Balme, K. Le Saux, M.E.H. Benbouzid, J.F. Charpentier and F. Hauville, "A simulation model for the evaluation of the electrical power potential harnessed by a marine current turbine," *IEEE Journal on Oceanic Engineering*, vol. 32, n°4, pp. 786-797, October 2007.

[2] *Technical Report*, Groupe 12A, *Les Hydroliennes*, Projet ADEM1 (in French):   http://www.heliciel.com/Library/Rapport%20hydrolienne.pdf, 2005.

[3] M. Leijon, H. Bernhoff, M. Berg and O. Ågren, "Economical considerations of renewable electric energy production—especially development of wave energy," *Renewable Energy*, vol. 28, n°8, p. 1201-1209, 2003.

[4] Z. Zhou, F. Scuiller, J.F. Charpentier, M.E.H. Benbouzid and T. Tang, "An Up-to-Date Review of Large Marine Tidal Current Turbine Technologies," In IEEE Power Electronics and Application Conference (Shanghai), China, November 2014

[5] S. Djebarri, J.F. Charpentier, F. Scuiller and M.E.H. Benbouzid, "Génératrice à aimants permanents à flux axial à grand diamètre avec entrefer immerge – Eléments de conception et analyse des performances pour un cahier des charges d'hydrolienne," *European Journal of Electrical Engineering*, vol. 16, n°2, pp. 145-176, 2013.

[6] J. Ribrant and L. Bertling, " Survey of Failures in Wind Power Systems With Focus on Swedish Wind Power Plants During 1997–2005 ," IEEE Trans. on energy Conversion, Vol 22 , n° 1, pp 167 - 173, March 2007.

[7] J.A. Baroudi, V. Dinavahi and A.M. Knight, "A review of power converter topologies for wind generators," *Renewable Energy*, vol. 32, n°14, p. 2369-2385, 2007.

[8] Z. Zhou, M.E.H. Benbouzid, J.F. Charpentier, F. Scuiller and T. Tang, "A review of energy storage technologies for marine current energy systems," *Renewable & Sustainable Energy Reviews*, vol. 18, pp. 390-400, February 2013.

[9] Y. Amirat, M.E.H. Benbouzid, E. Al-Ahmar, B. Bensaker and S. Turri, "A brief status on condition monitoring and fault diagnosis in wind energy conversion systems," *Renewable & Sustainable Energy Reviews*, vol. 3, n°9, pp. 2629-2636, December 2009.

[10] Z. Zhou, F. Scuiller, J.F. Charpentier, M.E.H. Benbouzid and T. Tang, "Power Control of a Nonpitchable PMSG-Based Marine Current Turbine at Overrated Current speed With Flux-Weakeninig Strategy," IEEE Journal of Oceanic Engineering, Vol PP, Issue 99, Octobre 2014.

[11] S. Djebarri,.;J.F. Charpentier.;F. Scuiller;M. Benbouzid, "A systemic design methodology of PM generators for fixed-pitch marine current turbines," in proceedings of International Conference on Green Energy, 2014, vol., no., pp.32,37, 25-27 March 2014.

[12] A.S. Bahaj, A.F. Molland, J.R. Chaplin and W.M. J. Batten, "Power and thrust measurements of marine current turbines under various hydrodynamic flow conditions in a cavitation tunnel and a towing tank," *Renewable Energy,*, vol. 32, n°3, p. 407-426, 2007.

[13] Siemens SWT-6.0-154 6MW, *Technical Report*. available at http://www.swe.siemens.com/spain/web/es/energy/energias_renovables/eo lica/Documents/6MW_direct_drive_offshore_wind_turbine.pdf   (last acceced: December 2013).

[14] S. Djebarri, J.F. Charpentier, F. Scuiller, M.E.H. Benbouzid and S. Guemard, "Rough design of a double-stator axial flux permanent magnet generator for a rim-driven marine current turbine," *in Proceedings of the 2012 IEEE ISIE*, Hangzhou (China), pp. 1450-1455, May 2012.

[15] L. Drouen, J. F. Charpentier, E. Semail and S. Clenet, "Study of an innovative electrical machine fitted to marine current turbines," *in Proceedings of the 2007 IEEE OCEANS*, Aberdeen (Scotland), pp. 1-6, June 2007.

[16] S. Chaithongsuk, B. Nahid-Mobarakeh, J.P. Caron, N. Takorabet, and F. Meibody-Tabar, "Optimal design of permanent magnet motors to improve field-weakening performances in variable speed drives," IEEE Trans. Industrial Electronics, vol. 59, n°6, pp. 2484-2494, Jun. 2012

[17] J. Chen & D. Jiang, "Study on modeling and simulation of non-grid-connected wind turbine," In IEEE World Non-Grid-Connected Wind Power and Energy Conference (WNWEC), Nanjing, pp. 1-5, September 2009

[18] J. G. SLOOTWEG, S. W. H. DE HAAN, H. POLINDER, "General model for representing variable speed wind turbines in power system dynamics simulations," Power Systems, IEEE Transactions on, vol. 18, no 1, p. 144-151, 2003